Qualification of PBF-LB/P manufactured TPU Components for Media-Tight Applications

Paper Number (C000297)

Vera Rothmund[*1,6], Sebastian Bremen[1,4,5], Carolina Bittencourt Wang[1], Martin Launhardt[2], Volker Junior[3]

[1]*Fraunhofer Institute for Laser Technology ILT, Aachen, Germany*
[2]*Launhardt GmbH, Zülpich, Germany*
[3]*phoenix GmbH & Co. KG, Munich, Germany*
[4] *Mechanical Engineering and Mechatronics, University of Applied Science Aachen, Germany*
[5]*Institut für werkzeuglose Fertigung GmbH, Aachen, Germany*
[6]*Chair for Laser Technology LLT, RWTH Aachen University, Aachen, Germany*
[*]*Corresponding author's e-mail: vera.rothmund@ilt.fraunhofer.de*

Abstract: Additive manufactured thermoplastic polyurethane (TPU) components for applications such as vacuum grippers or seals are of increasing interest. Porosity and surface roughness remaining from the PBF-LB/P process pose significant challenges to sealing performance. This work aims to evaluate the suitability of PBF-LB/P-manufactured TPU components for sealing applications, with a focus on the influence of PBF-LB/P process chamber temperature and chemical smoothing. Test specimens were produced using *Monkey TPU 50* (Launhardt GmbH) on a Sinterit Lisa X machine varying process chamber temperatures from 105 °C to 120 °C. Mechanical properties (hardness, tear resistance, compression set) and surface characteristics (roughness) were evaluated before and after chemical smoothing. Performance was assessed via qualitative overpressure and negative pressure tests. Chemical smoothing enables the use of PBF-LB/P TPU components in media-tight applications by eliminating surface porosity and closing the part surface. In addition to lowering roughness, smoothing alters all other investigated properties: Shore-A hardness and tear resistance increase, while compression set also rises. PBF-LB/P TPU components can potentially meet media-tightness requirements when combined with chemical post-processing. The method enables functional sealing parts like vacuum grippers with tailored geometries. Future work should investigate cyclic and dynamic sealing performance to assess long-term application suitability.

Keywords: additive manufacturing, PBF-LB/P, SLS, TPU, spherical powder, chemical smoothing, porosity, sealing applications, compression set, tear resistance

1. Introduction

Thermoplastic polyurethane (TPU) is an elastomeric polymer valued for its flexibility, abrasion resistance, chemical stability, and resilience under dynamic load. These characteristics have made TPU a popular material for applications across a wide range of industries, including wearable devices, damping components, footwear, medical orthoses, and protective housings. With the continued rise of additive manufacturing (AM) for enduse parts, there is increasing interest in using TPU to produce customized, small-batch, or geometrically complex parts that benefit from its elastic behavior such as seals or vacuum grippers.

Powder Bed Fusion with Laser Beam for Polymers (PBF-LB/P) – also referred to as Selective Laser Sintering (SLS) – is particularly known for additively manufacturing complex, support-free geometries. This key advantage applies across all printable polymer powders such as polyamide (PA) and TPU [1–4]. Support structures are not required in PBF-LB/P because the surrounding unsintered powder acts as a natural support during the print process, stabilizing overhangs and complex features without additional material.

One potentially emerging use case for PBF-LB/P TPU lies in the production of sealing elements and vacuum grippers, particularly in fields such as automation, food handling, and automotive assembly. These components must conform to complex surfaces, maintain media tightness under pressure differentials, and in some cases meet specific hygienic or mechanical standards.

Vacuum grippers are typically produced using injection molding, which is economical for standardized geometries and offers good durability. However, when specialized gripper shapes are needed to handle sensitive or irregular parts, mold-based manufacturing becomes inflexible and uneconomical. Sealing elements, especially in small series or with delicate features, are sometimes manufactured using vat photopolymerization (VPP) due to their high resolution and surface quality. Yet, VPP typically requires manual removal of support structures, a time-consuming and difficult-to-automate step that limits scalability.

PBF-LB/P overcomes this by enabling the direct fabrication of both component types without supports, making it attractive for custom-shaped sealing and gripping

applications. However, TPU parts produced via this process exhibit residual porosity and surface roughness due to the material's low melt viscosity. This limits their use in media-tight applications, where even small defects can lead to leakage and functional failure.

A promising solution is chemical smoothing, a post-processing method that uses solvent vapor to selectively liquidify and reflow the outer surface of the part. This treatment eliminates surface porosity, reduces roughness, and creates a closed, media-tight skin – all while requiring minimal manual intervention compared to support removal in other AM processes. As such, it represents a viable industrial approach to enabling leak-tight TPU parts made by PBF-LB/P.

Despite these capabilities, the production of soft, sealing-capable TPU parts via PBF-LB/P has been scarcely investigated. One key reason is the limited availability of low-hardness TPU powders in the past.

In this study, "Monkey TPU 50" (Launhardt GmbH), a newly developed soft TPU powder for PBF-LB/P, is evaluated. The influence of process chamber temperature in the PBF-LB/P machine and subsequent chemical smoothing on key mechanical and sealing-relevant properties is assessed. The goal is to determine whether this material-process combination can meet the functional requirements for media-tight sealing and vacuum gripping.

2. Background and Related Work

Despite its potential, additively manufactured TPU faces challenges that are critical for sealing applications. The porous microstructure and characteristic grainy surface texture of PBF-LB/P parts mean they are not inherently media-tight which means gas or liquid can permeate through interconnected pores. A well-known issue with PBF-LB/P [5]. Even under optimized sintering conditions, voids remain between fused powder particles; researchers have reported porosity levels on the order of ~5–20% in PBF-LB/P TPU parts produced with typical parameters [6]. Practical experience shows that SLS-printed polymer parts may require wall thicknesses of ~2 mm or more to hold water without leakage. Leaks tend to initiate at sealing surfaces due to the intrinsic surface roughness of PBF-LB/P components [7]. Under highly tuned conditions, porosity can be reduced substantially, e.g. to below 1% [6], but surface asperities prevent a perfect seal at contact interfaces [5,7].

Prior research has explored various strategies to improve the density and properties of PBF-LB/P TPU parts. For example, Dadbakhsh *et al.* investigated how powder particle shape and size influence PBF-LB/P processability and found that using high-quality (e.g. spherical) powder leads to better fusion and mechanical strength in TPU prints [8]. Likewise, Xu *et al.* reported that increasing the powder bed temperature and laser energy input can enhance layer bonding in TPU, thereby reducing porosity and improving tensile properties [9]. Dadbakhsh *et al.* analyzed multiple TPU grades and demonstrated that PBF-LB/P can indeed produce TPU components, but noted the aforementioned high porosity in unsintered regions and potential material thermal degradation when processing conditions are not optimal [8]. Overall, these studies underscore that powder characteristics and PBF-LB/P parameters significantly affect part quality [6]. Optimizing these parameters can yield nearly fully dense TPU parts in the best cases [6], although a completely pore-free part is seldom achieved without further treatment. Moreover, the as-sintered surfaces of TPU components remain rough at the microscale, which is problematic for sealing even if the bulk is dense [7].

To overcome these limitations, researchers and industry players have turned to post-processing techniques that seal the surface and remove porosity. One effective approach is chemical smoothing (also known as vapor smoothing or chemical polishing) of PBF-LB/P parts [10]. The result is a dramatically smoother, closed surface. Formlabs and AMT report that chemical smoothing can reduce the average surface roughness of PBF-LB/P prints by about 72–81%, yielding a finish and texture comparable to injection-molded plastic [11]. Crucially for functionality, the smoothing process seals any surface pores, thereby preventing liquid or gas from penetrating the part's shell [12]. Industrial references indicate that this technique enables additively manufactured TPU parts to meet media tightness requirements. For example, PBF-LB/P TPU parts can be used as seals in automotive and electronics, effectively achieving requirements for practical applications [13]. Smoothing can thus unlock sealing applications for additively manufactured TPU that would otherwise be infeasible with the rough, porous as-sintered surface.

Another benefit of chemical smoothing is that it can improve a part's mechanical performance or at least cause no significant deterioration. Because the solvent treatment only alters the outer layers, the core material and dimensions remain essentially unchanged [11]. Studies have shown that key properties like tensile strength are retained after smoothing, while elongation at break may even increase [9] due to the removal of surface flaws [12]. On the other hand, the process does slightly modify surface-dependent properties e.g. shore hardness or compression behavior. In general, literature suggests that a properly executed chemical smoothing treatment achieves its primary goals without compromising the part's integrity [11].

Given these advancements, the feasibility of additive manufactured TPU seals has started to be demonstrated. Notably, Ebel *et al.* (2024) recently produced fully additively manufactured hydraulic rod seals using TPU in the material extrusion (MEX) process and tested them under significant pressure and motion. Their results showed that printed seals could withstand fluid pressures up to 15 MPa in dynamic conditions before leakage, although the wear and sealing behavior differed from conventional injection molded seals [14]. This evidence confirms that, at least for short-term use, AM techniques can deliver functional seal components.

In summary, background research indicates that manufacturing TPU via PBF-LB/P offers great design flexibility and acceptable mechanical properties for elastomeric parts, but inherent porosity and surface roughness pose challenges for media-tight applications [5]. Prior work has addressed these issues by adjusting PBF-LB/P process parameters (e.g. higher bed temperatures, improved powder quality) and by applying post-process treatments like chemical smoothing to close the part surface [6,12]. These measures have been shown to substantially improve density, surface finish, and sealing capability in AM TPU parts. Building on this state of the art, the present work evaluates the suitability of PBF-LB/P TPU components for sealing applications, with particular focus on how process chamber temperature and a

chemical smoothing post-treatment affect the material's hardness, tear resistance, compression set, surface roughness, and ultimately its ability to form a leak-tight seal. The findings will help establish whether PBF-LB/P TPU, combined with appropriate post-processing, can meet the stringent demands of media-tight seals in practice.

3. Research Aim

The aim of this study is to investigate whether flexible, media-tight components can be reliably produced from TPU using the PBF-LB/P process in combination with chemical smoothing. The focus is on determining whether this process chain enables sufficient sealing performance and mechanical stability to qualify for functional applications such as seals and vacuum grippers.

By exploring different PBF-LB/P process chamber temperatures and applying vapor-based chemical smoothing, the study assesses how surface roughness, porosity, hardness, compression set, and tear resistance are affected.

4. Materials and Methods

To investigate the influence of PBF-LB/P process conditions and surface treatment on the mechanical and sealing relevant properties of TPU components, test specimens were produced using the PBF-LB/P process with the following four process chamber temperatures: 105 °C, 110 °C, 115 °C, and 120 °C. For each manufacturing condition, specimens were evaluated in two states: after sandblasting with a spherical abrasive (grain size 100–200 µm) and after additional chemical smoothing.

4.1 Material and Machine Setup

All specimens were fabricated from "Monkey TPU 50", a soft thermoplastic polyurethane powder developed and provided by Launhardt GmbH. Printing was performed on a commercially available Sinterit "Lisa X" PBF-LB/P system using standard settings provided by the software "Sinterit Studio", except for the process chamber temperature, which was varied across print jobs to assess its influence. A detailed list of process parameters can be found in Table 4 in the appendix.

Each print job included all required test geometries and was prepared with consistent part orientation and layout. The placement of the specimens on the printer's platform is shown in Fig. 1.

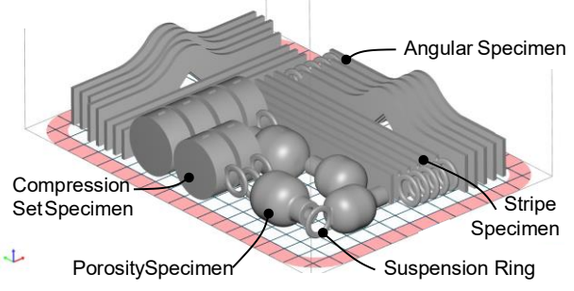

Fig. 1: Arrangement of specimens for each print job

4.2 Postprocessing

All printed specimens underwent a two-stage post-processing procedure. Initially, compressed air and sandblasting were used to remove residual powder. This step was performed for all samples to ensure a consistent starting condition.

From each print job produced, half of the specimens were subsequently subjected to chemical smoothing. Therefore, a suspension ring was added to the geometries as shown in Fig. 1. The chemical smoothing was carried out using a "PostPro SF50" vapor smoothing system (AMT, Sheffield, UK) in combination with the solvent "PostPro-Pure". The process involves thermal preconditioning of the parts, solvent vapor generation under reduced pressure, surface reflow via condensation, and final drying.

Due to the limited number of samples available, it was not possible to determine the best smoothing parameters for the corresponding PBF-LB/P process chamber temperatures. Consequently, potential effects of non-optimized parameters on the chemical smoothing outcome couldn't be ruled out in this study.

4.3 Test Methods

A set of mechanical and functional tests was performed to assess the influence of PBF-LB/P process chamber temperature and post-processing on the performance of the printed TPU specimens. The test methods, standards and corresponding sample type are summarized in Table 1.

Table 1 Overview of sample names, corresponding test types and quantities of samples

Sample Name	Test Type	Quantity of test samples (of which chemically smoothed)
Stripe Specimen	Tear Resistance (ISO 34-1)	10(5)
Angular Specimen	Tear Resistance (ISO 34-1)	10(5)
Compression Set Specimen	Compression Set (DIN ISO 815-1); Hardness (DIN ISO 48-4)	6(3)
Porosity Specimen (Wall thickness 3 mm)	Overpressure test	2(1)
Porosity Specimen (Wall thickness 1.5 mm)	Overpressure test	2(1)

Porosity and media-tightness were investigated using a combination of overpressure testing, negative pressure testing, scanning electron microscopy (SEM) and cross-section microscopy. For the overpressure test, each porosity specimen was connected to a standard workshop compressed air line using adhesive tape. The specimens were then submerged in water and pressurized internally at 600 to 800 kPa. The emergence of air bubbles indicated leakage. To complement these results, a negative pressure test was performed on vacuum gripper demonstrators of varying wall thicknesses and size made from the same TPU material. Connected to a manual vacuum pump, the grippers were qualitatively assessed for their ability to generate and maintain negative pressure under simulated functional conditions.

To gain additional insight into surface porosity and microstructural changes, SEM imaging was performed before and after chemical smoothing. Furthermore, the smoothing result was examined using cross-section microscopy.

Roughness was analyzed using optical profilometry. The roughness parameters R_a, S_a, R_z, and S_z were recorded on the flat surface of the compression set specimens. Measurements were taken in three conditions: after compressed air cleaning, after sandblasting, and after chemical smoothing.

Hardness was measured according to DIN ISO 48-4 with the following slight variation [15]: Lateral surfaces of the compression set specimens were used instead of cuboid geometry according to the beforementioned. Four measurements were taken on each side per sample and averaged out.

The compression set describes the material's ability to recover its original shape after prolonged mechanical compression. It was determined based on DIN ISO 815-1 [16] at room temperature for 24 hours. Subsequently, the same chemically smoothed specimens were examined analogously at 70 °C The test was performed on cylindrical specimens with a height of 12.5 mm and diameter of 29 mm.

Tear resistance was evaluated according to DIN ISO 34-1 [17] using angular and stripe shaped specimen geometries. Angular specimens assess crack initiation from notches, while stripe specimens evaluate uniform tear propagation, providing complementary insights. Tests were carried out on a universal testing machine at constant crosshead speed. Tear strength T_s was calculated as the maximum recorded force divided by specimen thickness. Evaluation followed Method B for multi-point diagrams.

5. Results

This section begins with an overview of the fabrication and post-processing results of the test specimens as irregularities occurred. It then presents the experimental results, structured category starting with porosity, followed by hardness, compression set, roughness, and tear resistance.

5.1 Sample Preparation

All test specimens were built simultaneously for each process temperature on a single platform to ensure consistent process conditions across sample types. As shown in Fig. 1, the print layout included parts for all mechanical and functional tests. The specimens were arranged in rows and oriented on the edge on the build platform to maximize packing density and layer consistency.

For the specimens intended for chemical smoothing, the standard geometries were modified by adding a suspension ring to a nonfunctional surface to allow the parts to be hung freely in the vapor chamber.

The printed parts generally exhibited good quality, with well-formed features and clean surfaces across most geometries. A notable exception occurred in the 3 mm porosity test specimen printed at 105 °C, which showed major defects. Visible warping and layer misalignment indicated that the part had shifted within the powder bed during the print, leading to significant geometric distortion.

Powder removal was performed in two steps using compressed air followed by sandblasting. While this approach proved effective overall, prints produced at higher chamber temperatures resulted in a denser and more cohesive powder cake, causing partially sintered powder to adhere more strongly to the parts after cleaning with compressed air. At 120 °C, it became apparent that further increases in chamber temperature could lead to excessively sintered powder beds, potentially inhibiting part removal without mechanical damage. This indicates a practical upper limit for process temperature in terms of depowdering and part recovery.

During chemical smoothing, specimens were initially suspended using small, printed rings. In the first chemically smoothed batch (110 °C print), these suspension rings tore during processing, likely due to thermal softening and solvent exposure, causing the parts to fall to the chamber floor. For all subsequent batches the specimens were pierced with wire and hung directly through the test body.

All chemically smoothed specimens with wall thickness ≤ 2 mm were affected by notable shape distortion, and several samples had to be manually separated using a scalpel, which introduced surface defects. One stripe specimen from the 110 °C print was irreversibly damaged and therefore couldn't be tested. The condition of all chemically smoothed parts prior to separation is shown in Fig. 2.

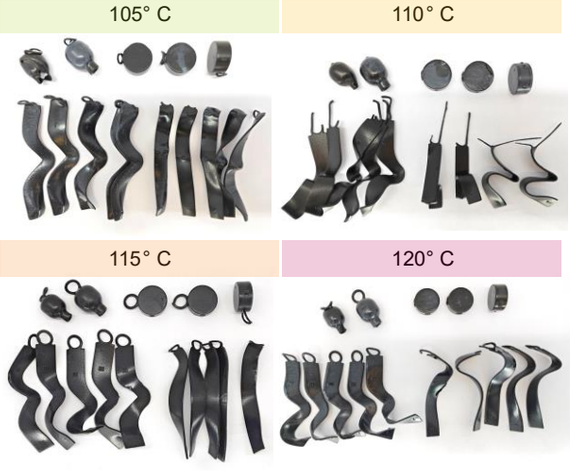

Fig. 2: chemically smoothed samples

5.2 Porosity Investigation

To assess the influence of chemical smoothing on porosity and sealing behavior, qualitative leakage tests were performed on TPU specimens with wall thicknesses of 3 mm and 1.5 mm. However, due to damage and unexpected outcomes, not all planned tests could be carried out.

Leakage testing was performed in two stages, starting with the sandblasted 3 mm wall thickness porosity specimens. Compressed air was applied internally while the parts were submerged in water. The emergence of continuous air bubbles across the entire surface confirmed a high degree of open porosity.

Based on these results, the sandblasted 1.5 mm specimens were excluded from testing under the assumption that their performance would be equal or worse due to reduced material thickness.

Subsequently, the chemically smoothed 3 mm wall thickness porosity specimens were tested. One specimen from 105 °C print showed visible warping after printing and retained open surface porosity even after chemical smoothing. For this reason it was excluded from leakage testing. Of the three remaining chemically smoothed specimens, two

exhibited local leakage, with air bubbles visibly escaping at sharp, inward-facing corners. This indicates that complex geometries may hinder effective surface closure during chemical smoothing. One smoothened specimen remained leak-tight for the entire test duration. Testing of the chemically smoothed 1.5 mm specimens was also omitted because all samples in this group showed significant deformation from post-processing, particularly near the pneumatic connection area.

The effectiveness of chemical smoothing in reducing surface porosity is clearly illustrated in Fig. 3. The SEM image on the left shows the sandblasted surface, characterized by partially sintered powder particles, voids, and a rough, porous structure. In contrast, the chemically smoothed surface (right) appears homogeneous and closed, with reflowed surface morphology and no visible open pores, indicating that the solvent vapor successfully sealed the outer layer.

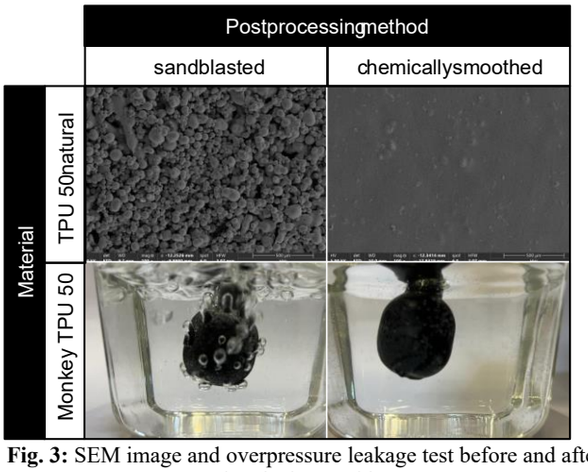

Fig. 3: SEM image and overpressure leakage test before and after chemical smoothing

Fig. 4, shows polished cross-sections of an angled specimen and a suspension ring in the chemically smoothed condition (120 °C print). It shows a continuous closed outer shell and a porous core without surface-connected porosity. These observations align with the behavior in the porosity test and the SEM Image after chemical smoothing.

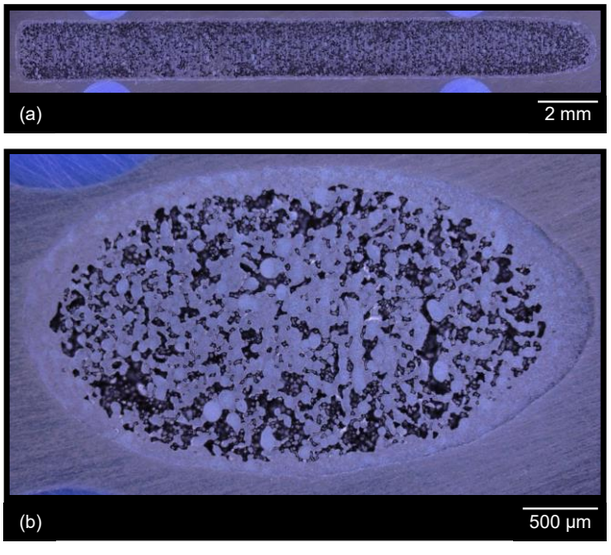

Fig. 4: Cross-sections from the 120 °C set after chemical smoothing: (a) angular specimen (b) suspension ring

Additionally, four vacuum gripper geometries were tested. Two were able to generate and hold negative pressure reliably. Both had a wall thickness of 2 mm and had undergone chemical smoothing. They reached a negative pressure level of approximately -66.6 kPa and were able to maintain this for 30 seconds. In contrast, the remaining two grippers with reduced wall thickness (≤1.5 mm) were unable to generate or hold a negative pressure. These findings support the assumption that wall thickness plays a critical role in leak-tightness.

5.3 Hardness Investigation

The Shore-A hardness of the TPU specimens shows a dependency on both the process chamber temperature and the post-processing condition. In general, higher process chamber temperatures lead to increased hardness in both sandblasted and chemically smoothed states. Additionally, chemically smoothed samples consistently exhibit slightly higher Shore-A values than their untreated counterparts across all PBF-LB/P process chamber temperatures (Fig. 5).

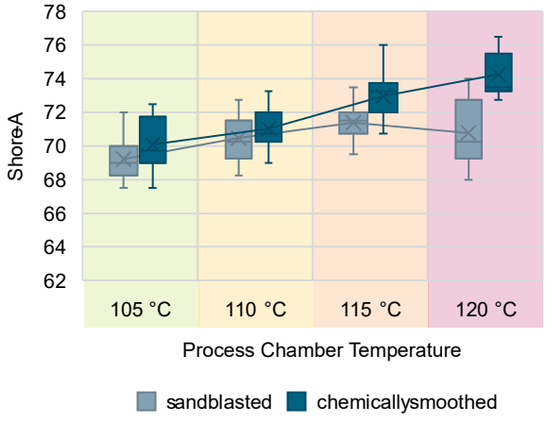

Fig. 5: Influence of process chamber temperature and surface treatment on hardness

At 105 °C, the average Shore-A hardness was 69 in the sandblasted state and 70 after chemical smoothing, corresponding to an increase of 1.3 %. At 110 °C, the values were 70 (sandblasted) and 70 (chemically smoothed), with an increase of 0.8 %. At 115 °C, hardness increased from 71 to 73, yielding a 2.2 % rise. At 120 °C, the average hardness was 71 before and 74 after chemical smoothing, corresponding to an increase of 4.9 %.

In addition, a linear relationship was observed between chamber temperature and hardness. Shore-A hardness increased by approximately 1 unit for every 5 K rise in PBF-LB/P process chamber temperature. The data point from the 120 °C print deviated markedly from this trend and from prior measurements for this material. They are therefore considered statistical outliers.

This trend is consistent with previously reported effects of chemical smoothing, where surface densification, pore sealing, and stress-induced stiffening contribute to higher measured surface hardness [18].

5.4 Roughness Investigation

Roughness is assessed based on the parameters R_a, S_a, R_z, and S_z. The results are presented in Fig. 6, and surface topographies are shown in false-color height maps in Fig. 7.

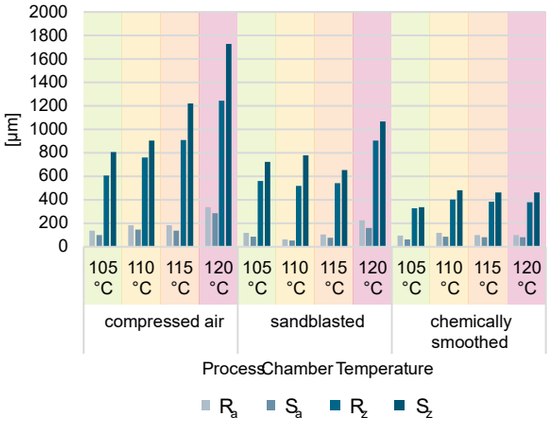

Fig. 6: Influence of process chamber temperature and surface treatment on roughness

The as-sintered specimens, cleaned only with compressed air, showed the highest surface roughness across all post-processing conditions. At 120 °C PBF-LB/P process chamber temperature, roughness values peaked with R_a = 334.7 µm and S_z = 1727.4 µm, indicating severe surface irregularities and partially sintered powder particles sticking to the parts. A clear increase in roughness with rising PBF-LB/P process chamber temperature was observed.

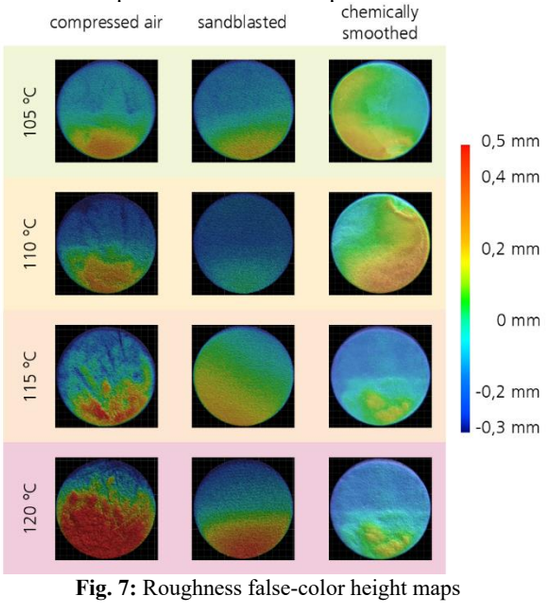

Fig. 7: Roughness false-color height maps

Sandblasting significantly reduced roughness at all temperatures. For example, at 115 °C, S_z dropped from over 1220.9 µm to 650.9 µm after sandblasting. However, deeper valleys and residual irregularities remained visible, especially at higher temperatures.

Chemical smoothing produced the lowest and most consistent surface roughness values. Across all PBF-LB/P process chamber temperatures, R_a ranged between 93 – 116 µm, and S_z was reduced to 338 - 479 µm. These values reflect a uniform and closed surface topography, largely independent of the initial PBF-LB/P process chamber temperature.

This trend is visually supported by the false-color maps which show a clear reduction in surface variation from left to right, especially at higher process temperatures. All individual R_a, S_a, R_z, and S_z values for each condition are listed in Table 5 in the appendix.

5.5 Tear Resistance Investigation

Tear resistance was investigated using stripe and angular specimens according to ISO 34-1 to capture both uniform tear propagation and crack initiation behavior. A detailed overview of the measured tear strength values (T_s) is provided in Table 2 (stripe specimens) and Table 3 (angular specimens), while Fig. 8 and Fig. 9 visualize the effect on both PBF-LB/P process chamber temperature and post processing method.

For stripe specimens, the sandblasted samples showed steadily increasing T_s values with rising PBF-LB/P process chamber temperature, reflecting improved cohesion in the sintered structure [19,20]. After chemical smoothing, T_s increased significantly across all PBF-LB/P process chamber temperatures. At lower PBF-LB/P process chamber temperatures, this effect was particularly strong, with T_s increasing by a factor of up to five compared to the untreated state. The smoothing effect became less pronounced at 120 °C, where the sandblasted samples already showed comparatively high tear strength, indicating that the higher PBF-LB/P process temperature alone already led to a more consolidated structure through the whole part.

This trend is clearly reflected by enveloping force-strain curves in Fig. 13 in the appendix, where chemically smoothed specimens reached higher peak loads. Sandblasted samples, in contrast, failed at lower forces and over shorter deformation.

Table 2 Influence of process chamber temperature and surface treatment on T_s - focus on crack propagation

Process chamber temperature	Average T_s [kN/m] Stripe Specimens	
	Sandblasted	Chemically Smoothed
105 °C	0,939	6,336
110 °C	1,469	6,799
115 °C	2,490	6,549
120 °C	3,725	5,582

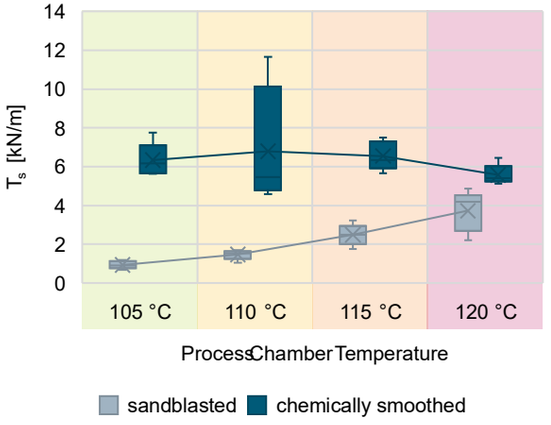

Fig. 8: Influence of process chamber temperature and surface treatment on tear resistance stripe specimens

For angular specimens, which simulate more realistic load situations including crack initiation and stress concentrations, the T_s values were consistently higher than for strip specimens. Again, chemical smoothing significantly improved the results for all process chamber temperatures. The mechanical behavior is illustrated by the enveloping curves in Fig. 14 in the appendix, where chemically smoothed specimens show a larger elastic deformation range, delayed failure and higher force peaks compared to their sandblasted counterparts.

Together, the results underline the beneficial effect of chemical smoothing on crack initiation and propagation resulting in higher tear resistance values, particularly for soft TPU materials processed at lower to moderate temperatures.

Table 3 Influence of process chamber temperature and surface treatment on T_s - focus on crack initiation

Process chamber temperature	Average T_s [kN/m] Angular Specimen	
	Sandblasted	Chemically Smoothed
105 °C	10,635	25,502
110 °C	18,751	32,591
115 °C	22,040	35,882
120 °C	29,084	32,346

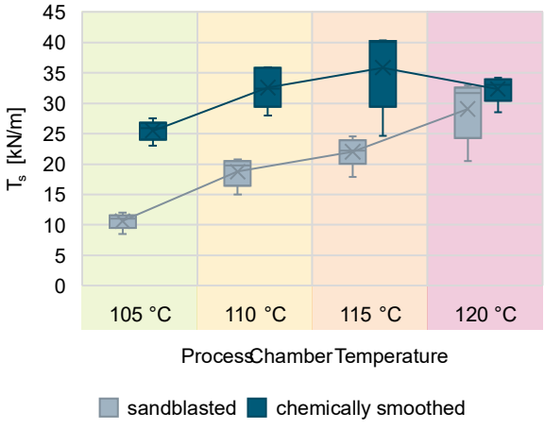

Fig. 9: Influence of process chamber temperature and surface treatment on tear resistance angular specimens

5.6 Compression Set Investigation

At first, room-temperature (20 °C) compression-set measurements were performed to establish a baseline and to enable comparison between sandblasted and chemically smoothed specimens. As shown in Fig. 10, compression set values increase with rising PBF-LB/P process chamber temperature in both sandblasted and chemically smoothed conditions. At every PBF-LB/P process temperature level, chemically smoothed specimens exhibit higher values than the untreated ones, which implies slight but tolerable loss of performance.

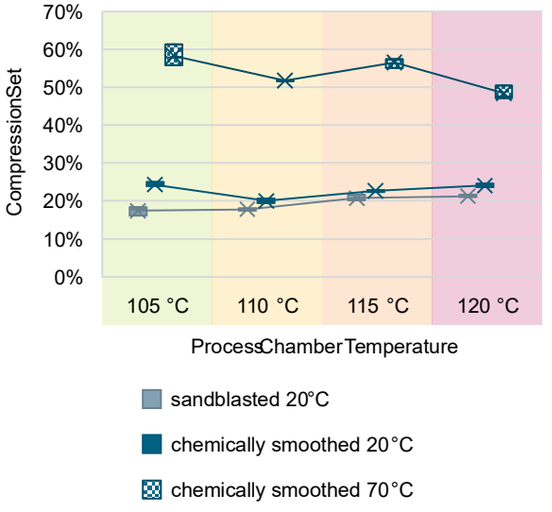

Fig. 10: Influence of process chamber temperature and surface treatment on compression set

On average, the compression set increased from 19.3 % in the sandblasted condition to 22.8 % after chemical smoothing, corresponding to a mean increase of 3.5 percentage points. The largest increase was observed at 105 °C, where values rose from 17.4 % to 24.3 % (+6.9 %).

This increase in compression set suggests that chemical smoothing reduces the elastic recovery of the material. A likely explanation is surface modification caused by polymer reflow, densification, or residual stress formation during the solvent-based process, which can affect the material's

ability to return to its original shape after compression [11,21,22].

While the sandblasted samples show a relatively steady increase in compression set with temperature, the chemically smoothed specimens behave less consistently. The relatively high value at 105 °C and the lower value at 110 °C deviate from the overall trend. It remains unclear whether these deviations are due to material effects or procedural variation.

In addition to room-temperature testing, the chemically smoothed specimens were subsequently tested at an elevated temperature of 70 °C reusing the same specimens. The 70 °C values are uniformly much higher than the room-temperature results for the smoothed condition and show a non-monotonic dependence on the PBF-LB/P process chamber temperature:

A summary compression set measurements is provided in Table 6 in the appendix.

6. Discussion

The findings demonstrate that while surface porosity can be effectively reduced through chemical smoothing, complete media-tightness is not always achieved. Leakage was still observed in some specimens, particularly at sharp internal features, indicating that chemical smoothing success depends strongly on part geometry and local surface conditions. Additionally, although the surface appeared sealed, internal porosity likely remained due to the nature of the PBF-LB/P process and TPU's low melt viscosity.

The assessment of compression set at room temperature provides only limited insight into the long-term performance of TPU components in practical sealing applications. In industrial practice, recommended maximum compression set values are typically based on testing at elevated temperatures, often 70 °C or higher, since elastomeric materials experience significantly more pronounced and irreversible deformation under thermal and mechanical stress. The values determined at 70 °C within this study may be too high for certain use cases. Therefore, alternative post-processing routes and should be investigated with the explicit goal of achieving lower compression set at 70 °C. *Richter* emphasizes that even well below their thermal stability limits, elastomers can exhibit substantial permanent deformation when exposed to prolonged loading at increased temperatures [23].

A noticeable deviation was observed in the Shore-A hardness data at 120 °C, which breaks the otherwise consistent trend seen in previous studies. Typically, a linear increase in hardness is expected with rising PBF-LB/P process chamber temperatures. The unexpectedly low value at 120 °C is likely a statistical outlier and should not be over-interpreted without further validation through repeated measurements.

The improvements in tear resistance were particularly pronounced in the angled specimens, which are more sensitive to crack initiation and propagation and thus more representative of functional part behavior. It must be noted that the resistance to crack growth under cyclic or long-term load conditions remains unassessed.

The unusual mechanical behavior of one chemically smoothed angular specimen (Sample 3.2 from the 115° print) further underlines limitations of this study. As shown in Fig. 11, the specimen was first tested to high elongation of 100 mm without failure and then subjected to a second attempt with an extended displacement range to ensure failure. In this second attempt, the force initially rose in a nearly linear manner but dropped abruptly to near zero after reaching only about 60 N, well below the maximum force from the first attempt. Although no visible damage was apparent after the first attempt, the second attempt revealed an abrupt and early failure, with significantly lower load-bearing capacity. This suggests that internal damage or microstructural changes occurred during the first attempt, likely due to polymer chain rearrangement or localized yielding. TPU's viscoelastic character allows for temporary deformation recovery, but its ability to sustain repeated mechanical loads without degradation is limited. Reuse of components after major deformation should therefore be avoided, even in the absence of visible defects.

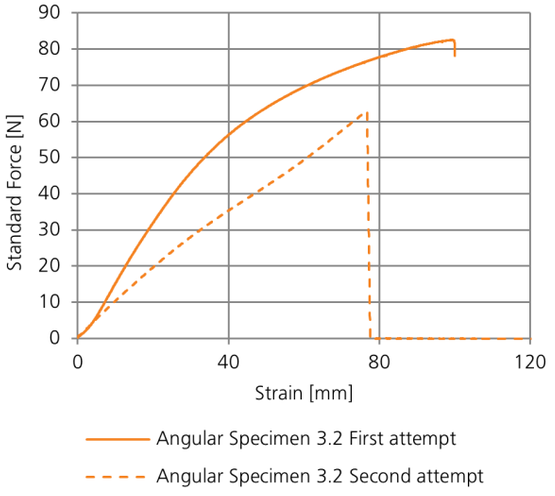

Fig. 11: Atypical crack initiation behavior – Force-strain curves of chemically smoothed angular specimen 3.2.

Regarding the sample preparation, the smoothing parameters were not fully matched to the specific PBF-LB/P process conditions and part geometries. In practice, chemical smoothing requires iterative optimization and tight control of exposure time and solvent intensity, tailored to the print conditions. As such optimization was beyond the scope of the present work, several specimens deformed during smoothing or were not evaluable. This limitation should be considered when interpreting the dataset.

7. Conclusion

PBF-LB/P TPU components for media-tight applications without chemical smoothing are not suitable for media tight applications such as seals or vacuum grippers, regardless of their wall thickness. However, chemical smoothing creates a closed surface that enables reliable media tightness. In this study, a functional vacuum gripper was successfully realized (Fig. 12), capable of generating stable negative pressure. Airtight components were also demonstrated in a qualitative overpressure test under water.

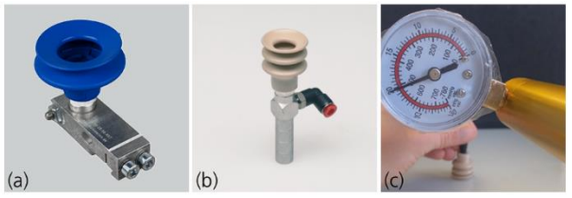

Fig. 12: Application "vacuum gripper"; a) conventional version b) PBF-LB/P manufactured TPU version c) while performance testing

Chemical smoothing additionally affects all material properties examined. For media-tight applications, most changes in values due to chemical smoothing are considered beneficial.

Shore-A Hardness increased slightly from 69 – 72 Shore A to 70 – 74 Shore A, while compression set increased from 17,4% < CS < 21,3% to 20,0% < CS < 24,3%.

Tear resistance behavior showed a complex response. Crack initiation threshold rose from 0,9 kN/m $<T_s<$ 3,7 kN/m to 5,6 kN/m $<T_s<$ 6,8 kN/m after chemical smoothing. Crack propagation resistance increased 10,6 kN/m $<T_s<$ 29 kN/m to 25,5 kN/m $<T_s<$ 35,9 kN/m after chemical smoothing.

Surface roughness was significantly reduced from 62,246 µm $<R_a<$ 226,032 to 93,159 µm $<R_a<$ 116,636 µm improving both sealing surface quality and consistency.

Sealing performance was demonstrated qualitatively and quantitatively: In overpressure testing, components withstood up to 600 to 800 kPa without leakage. In negative pressure testing, a level of -66.6 kPa was maintained for 30 seconds, indicating airtightness over time.

Geometry strongly influences the smoothing effect. A minimum wall thickness of 2 mm should not be undershot. Small radii should be avoided to ensure sufficient coverage with the solvent and, consequently, complete surface sealing.

Based on the findings PBF-LB/P of this study TPU components show great potential for use in media-tight applications such as vacuum grippers or seals with complex geometries. Different harnesses can be achieved and remain after chemical smoothing but more investigations are necessary in general and for specific operating conditions.

8. Outlook and Recommendations

The presented results reflect a conservative assessment. With finely tuned post-processing tailored to the material and geometry, the sealing performance of chemically smoothed TPU components may be further improved**.**

To further validate the suitability of chemically smoothed TPU components for sealing and gripping applications, future investigations should focus on long-term performance under realistic environmental and mechanical conditions.

The internal porosity of PBF-LB/P TPU parts remains largely unexplored and could critically influence media tightness and mechanical durability. Methods such as micro-CT imaging could be employed to analyze internal pore distribution and morphology. This could be embedded into a comprehensive design study.

Since chemical smoothing primarily affects the surface, any mechanical damage or abrasion may significantly compromise media-tightness. Future work should explore infiltration-based or hybrid techniques to improve internal sealing, especially for applications involving wear or repeated contact.

Finally, the performance of TPU under cyclic mechanical loads and dynamic sealing scenarios should be addressed to evaluate long-term structural integrity and enable reliable design criteria for flexible, media-tight components.

Acknowledgments

This work was carried out as part of the "SLSElasto" (FKZ: 03XP0466D) project, funded by the German Federal Ministry of Education and Research (BMBF) under the "KMU-innovativ" program.

The results presented were made possible with the support of the project partners: Launhardt GmbH (launhardt), rapid product manufacturing GmbH (rpm), phoenix GmbH & Co. KG (phoenix), and AGS Automation Greifsysteme Schwope GmbH (AGS). Special thanks also go to IwF (Institut für werkzeuglose Fertigung GmbH) for providing the LisaX-system used for the production of the test specimen.

Appendixes

Table 4: Parameter list

Parameter	Unit	"LAMP2025 I"	"LAMP2025 II"	"LAMP2025 III"	"LAMP2025 IIII"
Material		Monkey TPU	Monkey TPU	Monkey TPU	Monkey TPU
Machine Type		Sinterit Lisa X	Sinterit Lisa X	Sinterit Lisa X	Sinterit Lisa X
Date		09/04/2025	10/04/2025	11/04/2025	14/04/2025
Refresh Rate		100 wt.% (new powder)	50/50 wt.% (new/used powder)	50/50 wt.% (new/used powder)	50/50 wt.% (new/used powder)
Nitrogen usage		no	no	no	no
Layer Thickness	µm	100	100	100	100
Process Chamber Temperature	°C	105	110	115	120
Feed Bed Temperature	°C	105	105	105	105
Cylinder Temperature	°C	105	105	105	105
Piston Temperature	°C	105	105	105	105
Laser Power	W	30	30	30	30
Laser Power Ratio		1	1	1	1
Energy Scale		1,44	1,44	1,44	1,44
Max energy per cm³, infilll	J/cm³	150	150	150	150
Const energy, infill	J/cm³	0,15	0,15	0,15	0,15
Max power depth, infill	mm	2,3	2,3	2,3	2,3
Max energy per cm³, perimeters	J/cm³	70	70	70	70
Const energy, perimeters	J/cm³	0,5	0,5	0,5	0,5
Max power depth, perimeters	mm	2	2	2	2

Table 5: Roughness Values

Process chamber temperature	Surface	Roughness Values			
		R_a	S_a	R_z	S_z
105 °C	Compressed air	134,981	97,726	606,432	804,200
105 °C	Sandblasting	116,379	87,005	559,931	721,800
105 °C	Chemically Smoothed	93,159	62,497	324,864	338,600
110 °C	Compressed air	181,88	145,431	761,184	905,800
110 °C	Sandblasting	62,246	54,562	516,285	777,600
110 °C	Chemically Smoothed	116,636	85,520	401,414	479,900
115 °C	Compressed air	183,792	137,665	906,756	1220,900
115 °C	Sandblasting	105,720	74,511	541,140	650,900
115 °C	Chemically Smoothed	97,436	78,442	385,081	463,500
120 °C	Compressed air	334,710	286,983	1245,107	1727,400
120 °C	Sandblasting	226,032	159,288	904,579	1068,400
120 °C	Chemically Smoothed	98,174	78,086	380,478	464,000

Fig. 13: Enveloping force-strain curves from angular specimens of tear resistance investigation

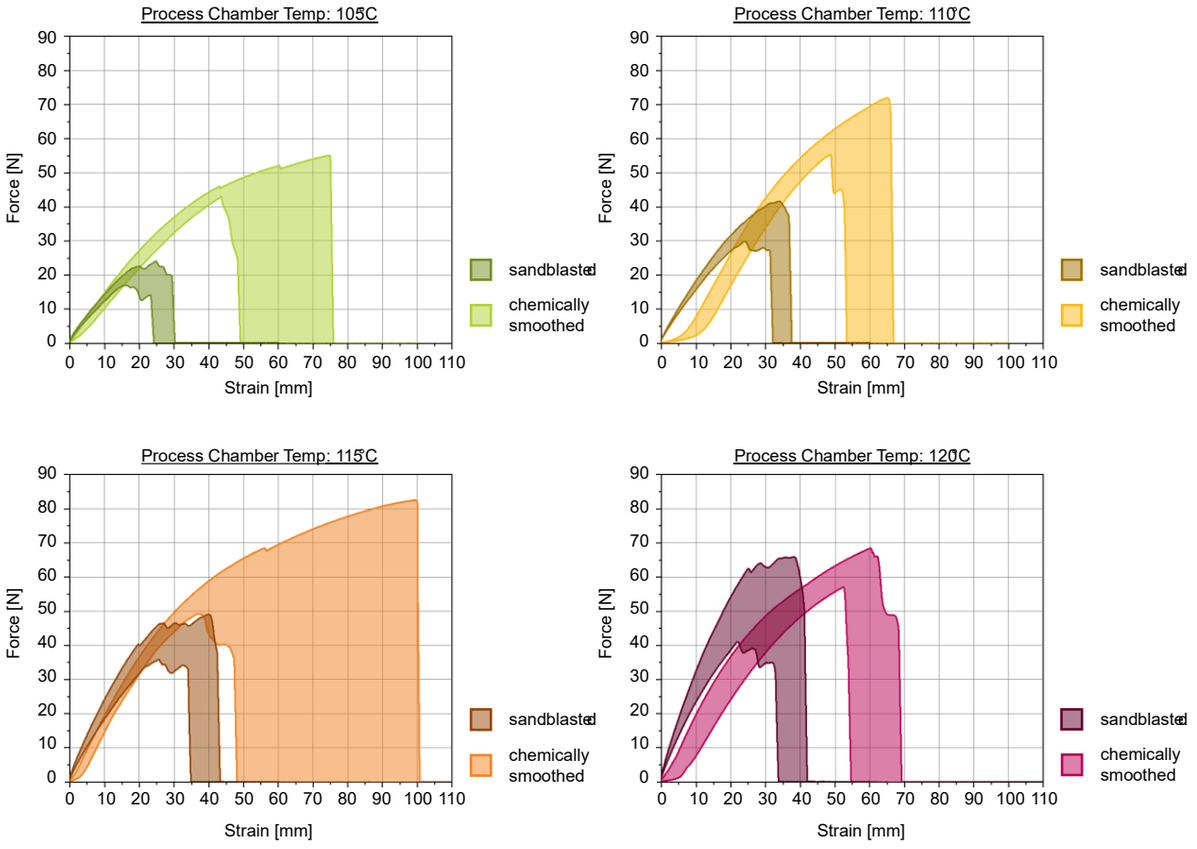

Fig. 14: Enveloping force-strain curves from stripe specimens of tear resistance investigation

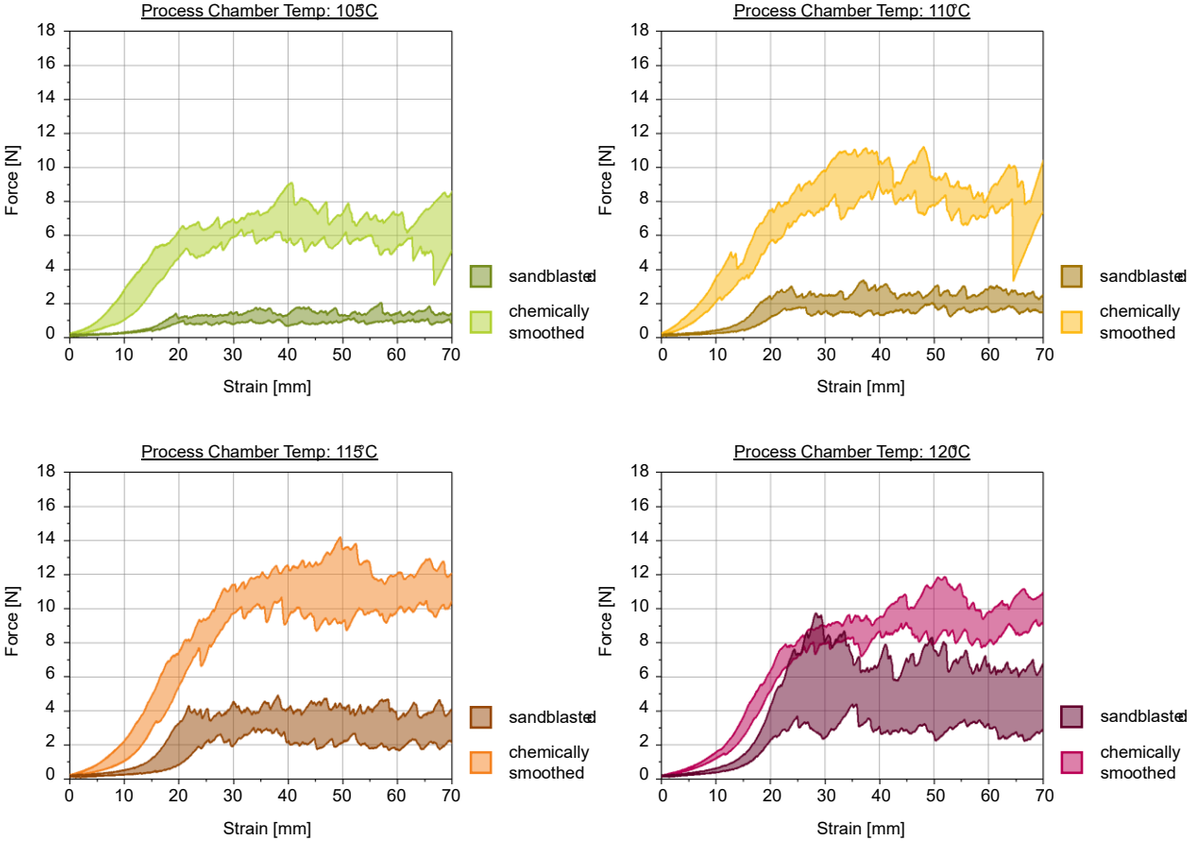

Table 6: Compression set calculated values

Process chamber temperature	Sand-blasted 20°C	Chemically Smoothed 20°C	Chemically Smoothed 70°C
105 °C	17,4%	24,3%	58,3%
110 °C	17,8%	20,0%	51,8%
115 °C	20,7%	22,7%	56,6%
120 °C	21,3%	24,1%	48,5%
Average:	19,3%	22,8%	53,8%

References

[1] ISO/ASTM 52900:2021, Additive manufacturing — General principles — Fundamentals and vocabulary (52900) (Geneva / West Conshohocken: International Organization for Standardization / ASTM International, 2021).

[2] I. Gibson, D. Rosen, B. Stucker and M. Khorasani, Additive Manufacturing TechnologiesCham: Springer International Publishing, 2021.

[3] J.-P. Kruth, P. Mercelis, J. van Vaerenbergh, L. Froyen and M. Rombouts, Binding mechanisms in selective laser sintering and selective laser melting, Rapid Prototyping Journal, vol. 11, 2005, 26-36. https://doi.org/10.1108/13552540510573365.

[4] A. Gebhardt, ed., Additive Fertigungsverfahren (München: Carl Hanser Verlag GmbH & Co. KG, 2016).

[5] FacFox Docs, Introduction to SLS 3D printing, [Online]. Available: https://facfox.com/docs/kb/introduction-to-sls-3d-printing. [Accessed 12 June 2025].

[6] C. Morano and L. Pagnotta, Additive Manufactured Parts Produced Using Selective Laser Sintering Technology. Comparison between Porosity of Pure and Blended Polymers, Polymers, vol. 15, 2023. https://doi.org/10.3390/polym15224446.

[7] Xometry Pro, Is it possible to print waterproof parts with SLS?, [Online]. Available: https://xometry.pro/de/topic/ist-es-moglich-wasserfeste-teile-mit-sls-zu-drucken.

[8] S. Dadbakhsh, L. Verbelen, T. Vandeputte, D. Strobbe, P. van Puyvelde and J.-P. Kruth, Effect of Powder Size and Shape on the SLS Processability and Mechanical Properties of a TPU Elastomer, Physics Procedia, vol. 83, 2016, 971-980. https://doi.org/10.1016/j.phpro.2016.08.102.

[9] T. Xu, W. Shen, X. Lin and Y. M. Xie, Mechanical Properties of Additively Manufactured Thermoplastic Polyurethane (TPU) Material Affected by Various Processing Parameters, Polymers, vol. 12, 2020. https://doi.org/10.3390/polym12123010.

[10] Sculpteo, Complete guide to Selective Laser Sintering (SLS), [Online]. Available: https://www.sculpteo.com/en/3d-learning-hub/3d-printing-technologies-and-processes/selective-laser-sintering.

[11] Formlabs GmbH, Leitfaden zum chemischen Dampfglätten für den SLS-3D-Druck, [Online]. Available: https://formlabs.com/de/blog/vapor-smoothing-sls-3d-printed-parts.

[12] Forerunner 3D, Vapor Smoothing Finish Options For 3D Printed Parts, [Online]. Available: https://forerunner3d.com/vapor-smoothing-finish-options-for-3d-printed-parts.

[13] 1zu1 Prototypen GmbH & Co KG, Selective Laser Sintering flexible (SLS), [Online]. Available: https://www.1zu1prototypen.com/en/3d-printing/sls-flexible.htm.

[14] T. Ebel, T. Lankenau, L. Sundermann, K. Ottink, M. Graf, B. Klie and U. Giese, Functional testing of entirely additively manufactured two-component hydraulic rod seals made of TPU and NBR, Discover Mechanical Engineering, vol. 3, 2024. https://doi.org/10.1007/s44245-024-00034-x.

[15] DIN ISO 48-4:2018, Rubber, vulcanized or thermoplastic — Determination of hardness — Part 4: Indentation hardness by durometer method (Shore hardness) (48-4) (Berlin / Geneva: Deutsches Institut für Normung / International Organization for Standardization, 2018).

[16] DIN ISO 815-1:2019, Rubber, vulcanized or thermoplastic — Determination of compression set — Part 1: At ambient or elevated temperatures (815-1) (Berlin / Geneva: Deutsches Institut für Normung / International Organization for Standardization, 2019).

[17] DIN ISO 34-1:2024, Rubber, vulcanized or thermoplastic — Determination of tear strength — Part 1: Trouser, angle and crescent test pieces (34-1) (Berlin / Geneva: Deutsches Institut für Normung / International Organization for Standardization, 2024).

[18] BASF Forward AM & AMT, Improving Ultrasint® TPU01 part properties by PostPro® vapour smoothing.

[19] BASF 3D Printing Solutions GmbH, Technical Data Sheet for Ultrasint® TPU88A, 2021.

[20] BASF 3D Printing Solutions GmbH, Technical Data Sheet for Ultrasint® TPU01, 2021.

[21] U. Blobner and Richter B., Druckverformungsrestprüfung (DVR-Prüfung). Prüftechnische Grundlagen und Empfehlungen für die praktische Anwendung, Fachwissen Prüfverfahren für Elastomere, 2015.

[22] S. Connor, R. Goodridge and I. Maskery, The effect of inter- and intra-layer delay time on TPU parts fabricated by laser powder bed fusion, Progress in Additive Manufacturing, 2025. https://doi.org/10.1007/s40964-024-00933-1.

[23] B. Richter, O-Ring as Standardized Component – Commentary on ISO 3601-5, 2015.